Fatigue strength of concrete-filled grillage decks

Autor(en): **Maeda, Y. / Kushida, K. / Matsui, S.**

Objekttyp: **Article**

Zeitschrift: **IABSE reports = Rapports AIPC = IVBH Berichte**

Band (Jahr): **37 (1982)**

PDF erstellt am: **17.09.2024**

Persistenter Link: https://doi.org/10.5169/seals-28961

Fatigue Strength of Concrete-Filled Grillage Decks

Résistance à la fatigue des tabliers en grille de poutres enrobées de béton

Ermüdungsfestigkeit von ausbetonierten Stahlgitterrosten

Y. MAEDA
Professor
Osaka University
Suita, Osaka, Japan

S. MATSUI
Assistant Professor
Osaka University
Suita, Osaka, Japan

K. KUSHIDA
Head of Design Section
Kobe Steel Co., Ltd
Wakihama, Kobo, Japan

SUMMARY

Although the concrete-filled, steel grillage is a popular form of highway bridge deck, there is little information available on its fatigue strength. With this in mind, three sets of fatigue tests were carried out. The test procedure and results are presented and the fatigue strength of I beams in the floor, including the effect of the infill concrete, is discussed. On the basis of the discussion the fatigue security of an actual bridge is evaluated and some recommendations made for floor design.

RESUME

Bien que les tabliers de ponts-routes mixtes constitués d'une grille de poutres métalliques enrobées de béton soient très répandus, il y a actuellement peu d'information sur leur résistance à la fatigue. Dans cet esprit, trois séries d'essais de fatigue ont été effectués. Ce rapport présente le dispositif d'essai et les résultats, ainsi qu'une discussion sur la résistance à la fatigue des poutres en double-té incorporée dans le tablier, en incluant l'effet du béton. Sur la base de cette discussion, on évalue la sécurité à la fatigue des ponts existants et on propose quelques recommandations pour le dimensionnement de ce type de tabliers.

ZUSAMMENFASSUNG

Obwohl Fahrbahnplatten aus Beton aus gegossenen Stahlrosten weit verbreitet sind, ist noch wenig Information über ihr Ermüdungsverhalten vorhanden. Aus diesem Grund wurden drei Serien Ermüdungsversuche durchgeführt. Die Versuchsdurchführung sowie die Resultate werden vorgestellt und die Ermüdungsfestigkeit der in der Fahrbahnplatte einbetonierten I-Trägern diskutiert. Basierend auf diesen Ergebnissen wird einerseits die Sicherheit gegenüber Ermüdung einer bestehenden Brücke bestimmt und andererseits werden Empfehlungen für die Dimensionierung solcher Fahrbahnplatten vorgeschlagen.

1. INTRODUCTION

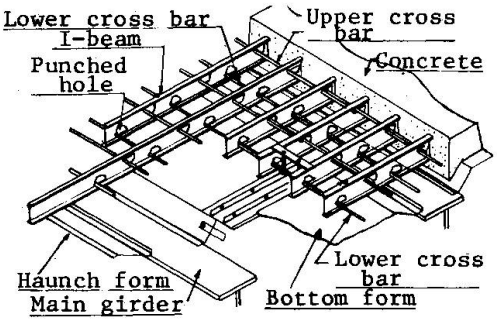

Fig.1 Sketch of floor.

Concrete Filled Steel Grating Floor is one of composite bridge decks. It has a large load-carrying capacity in spite of the thinner thickness than conventional RC-slabs[1]. The inner steel grid consists of specially rolled small I-beams and cross bars. The steel grid pannel as illustrated in Fig.1 is completely prefabricated at a shop. In Japan, a lot of serious damages of RC-slabs have been reported with a recent remarkable increase in traffic. Under these circumstances, the grating floors are getting to be frequently used not only for newly constructed bridges, but also for the replacement of damaged RC-slabs as seen in Fig.2, which shows the past records of use. The floor has already been recognized officially as a useful bridge deck. A design method, though it is yet in draft, is also proposed officially[2,3]. However, the authors have noticed that a more reasonable design method than the present proposed has to be established for the floors. There are two main problems to be considered, such as interaction between a steel grating and concrete from the point of plate behavior and fatigue strength of the floors. Regarding the former one, the authors have derived reasonable design bending moment formulas considering their orthotropic plate effects which would be caused by concrete cracking [4].

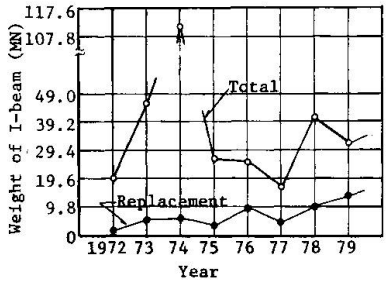

Fig.2 Past records of use of I-beams for bridge decks.

This paper covers discussions on fatigue of the floors. Fatigue fractures have been occasionally found in steel I-beams under large loading in our past labolatory tests. Generally, places of the fracture may be predicted to be located in the neighbor of edges of the loaded area as shown in Fig.3. Both bending and shear force in this region are very high. In addition, the I-beam has punched holes in the web, through which cross bars are placed, as shown in Fig.1. At the corner of the hole located in the region, a high stress occurs under simultaneous action of primary bending and secondary bending due to shear force as indicated in Fig.4. Furthermore, the effect of stress concentration due to the web opening is added to the previous stress. Accordingly, some points around the corner seem to be a crack initiation point. From the above experiences, three series of fatigue tests, such as isolated steel I-beam tests, concrete -encased I-beam tests and full-sized deck tests, were carried out. The first series are to clarify structural behaviors and fundamental fatigue features of the steel I-beams. The second series are to investigate the effects of concrete on the fatigue strength. The last are aimed at finding out the relation between the beam-type and the deck-type specimens. Through the tests the evaluation of the fatigue safety of the floor can be made.

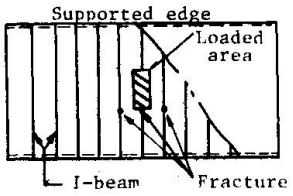

Fig.3 Cracking points in a deck.

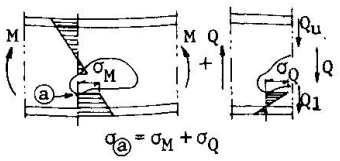

Fig.4 Stress at the corner of a hole.

2. DESCRIPTION OF SPECIMENS AND TEST PROCEDURES

2.1 Isolated Steel I-beam Tests

The two types of hole arrangements within an I-beam are typical for the practical usage. The first type has holes in a line along the lower side of the web. It is available in case upper cross bars are placed on the I-beams as shown in Fig.5(a). The second one has holes in a zigzag along the both sides of the web. It is use-

ful for thin decks because the upper cross bars also have to be placed through the web as seen in Fig.5(b). The first is named S-type and the second is W-type.

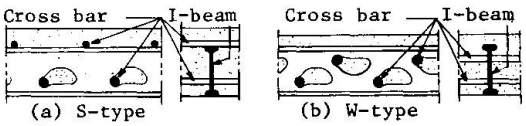

Fig.5 Types of I-beam.

Configurations of all the specimens are indicated in Fig.6. In the shop fabrication, cross bars are tack welded to I-beams so that the panel can have sufficient stiffness during its transportation and erection. Therefore, the influence of the welding on the fatigue strength at the welded points of the web is expected. The specimens of S-DB and W-DB in which 10 cm long deformed bars are welded, are also tested. Material properties of the I-beams are the same as those of structural carbon steel SS41 designated by the Japanese Industrial Standards. The static coupon tests of the steel showed 311 MPa, 483 MPa, 199 GPa, and 25.3 %, respectively, for its yielding stress, tensile strength, Young's modulus and elongation.

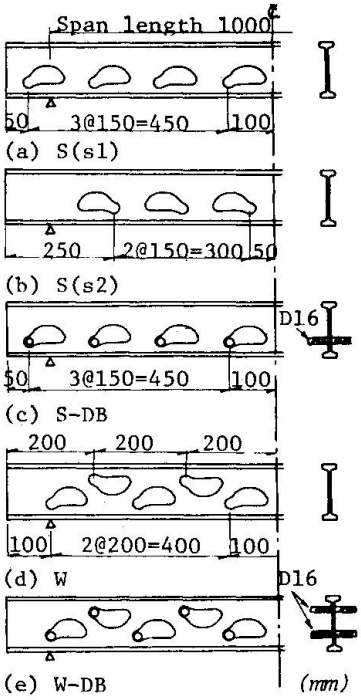

Fig.6 Isolated I-beam specimens.

A test apparatus for the beam-type specimens is illustrated in Fig.7. The span length is exactly 1.0 m. A great number of strain gauges of 2 mm or 5 mm gauge length were placed to measure strain distributions.

If the same repetition of loading is continued after the initiation of a crack, the crack will easily propagate to the bottom surface of the lower flange, and the I-beam loses its load-carrying capacity. Hereafter, such a phenomenon is called the fracture of an I-beam. The above mentioned test procedure gives only one kind of information for a single specimen. Therefore, the authors devised a procedure to obtain many data from a single specimen in order to save the time and the number of specimens by repairing each cracked hole. A repairing method by H.T.-bolts as shown in Fig.8 gave the most favorable results for the crack propagation arrest. As a matter of course, it was proved that the repairing scarcely gave an influence on the stress distribution at the adjoining cracking points. Thus, three or four data related to the life of initiation of a crack can be obtained from a single specimen. Afterward, one of the H.T.-bolts on the cracked points were released, and the repetition of the loading was continued until the fracture of the I-beam has been observed. By such a procedure, a remaining fatigue life up to the fracture can be also obtained.

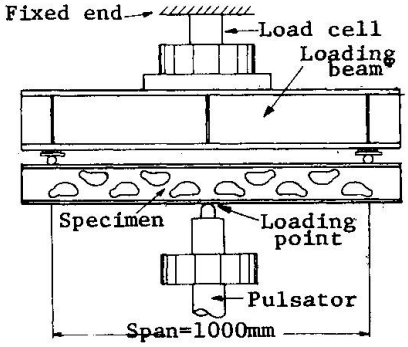

Fig.7 Test apparatus of beam test.

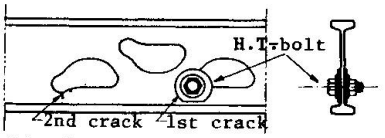

Fig.8 Repairing by H.T.-bolt.

2.2 Concrete -Encased I-beam Tests

The encased I-beam are essentially of S-, W-, S-DB-,and W-DB-types. The specimens are classified into three groups having the symbols of NC, NCC and COM as seen in Fig.9. NC means a specimen in which an I-beam is completely encased in concrete. NCC means a completely cast beam, but has artificial cracks in concrete up to the neutral axis of the composite section. These cracks are created by inserting thin plastic plates of 1 mm thickness and are uniformly distributed along the span with 10 cm to 15 cm intervals. COM means a composite beam which consists of one I-beam and concrete section only in the compression side.

In this series, the fatigue life is defined by the number of cycles of loading when a fracture of the I-beam has just occurred. It is named a fracture life.

2.3 Full-Sized Deck Tests

Two types of specimens as shown in Fig.10 were prepared. The decks are supported so that the two opposite edges can be simply supported and the other two be free. The deck span is 1.8 m. A single load is applied through a rectangular plate of 20 cm in length and 50 cm in width, which corresponds to the contact area of a rear wheel specified in the Specifications for Highway Bridges in Japan.

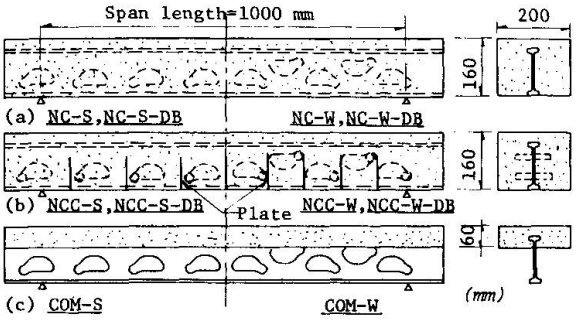

Fig.9 Concrete -encased I-beam specimens.

Since it is impossible to repair a cracked I-beam in a deck, a loading point is changed alternatively after each occurrence of fracture in the I-beam to obtain several data from a single specimen. In a deck specimen, since its load-carrying capacity does not decrease with only one fracture in the I-beam beneath a loading point, the fracture time of the I-beam was detected accurately by an electric instrument.

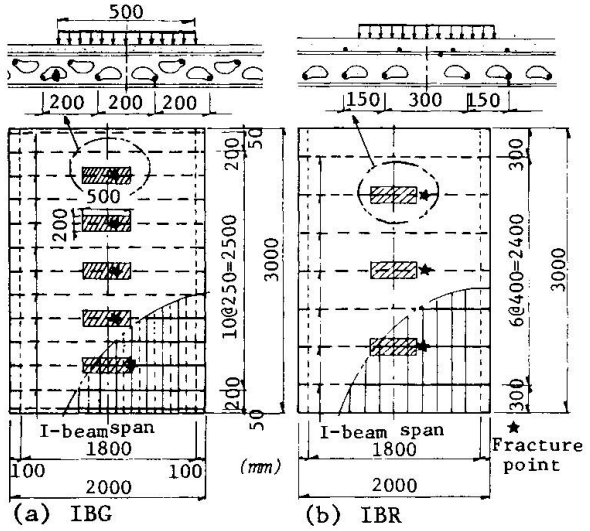

Fig.10 Deck specimens.

3. TEST RESULTS AND DISCUSSIONS

3.1 Fatigue Crack Patterns

Fig.11 shows patterns of fatigue cracks observed at the prototype I-beams. All cracking points in the tensile region are labeled by circled alphabets as seen in Fig.12. Hereafter, these labels will be used for explanations. When the circular part of a hole faces to a support, the first crack occurs at ⓐ of the nearest to a loading point. Then, fatigue cracks successively appear at the same part of outer holes with decreasing stresses. In the specimen S(s2), an initial cracks occurs at the point ⓑ, because stresses at ⓑ are higher than at ⓐ. In W-type specimen, the point ⓑ and ⓓ are also cracking points under a large load, since large stresses due to shear forces occur around these points. In W-DB-type which has deformed bars, fatigue cracks appear at the toe ⓒ of weld instead of ⓓ owing to the effects of heat and notch due to welding. The I-beams of the composite beams or decks showed the fracture of flanges caused by a crack from ⓐ as already shown in Fig.10.

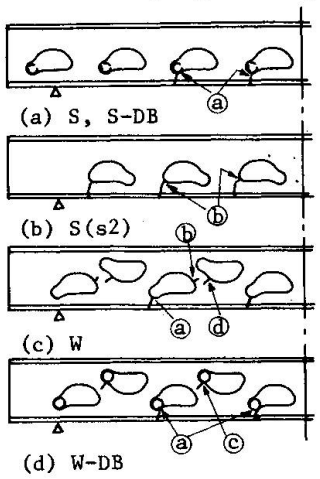

Fig.11 Fatigue crack pattern

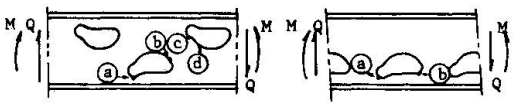

Fig.12 Labeling of cracking points.

3.2 Stress and Strain Distributions

Fig.13 shows a typical strain distribution measured at the lower flange of an I-beam. The zigzag distribution indicates how large an influence of secondary bending due to shear force is in an I-beam having web holes. Fig.14 is an example of stress distribution in the web of W-type beam by FEM. A large tensile stress appears in the neighbor of the points ⓐ, ⓑ, ⓒ and ⓓ. Especially, the stress at the point ⓐ is extremely high proving

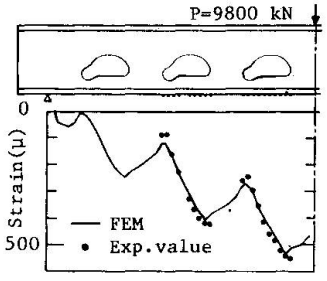

Fig.13 Distribution of strain on the bottom surface of a tensile flange of S-type beam.

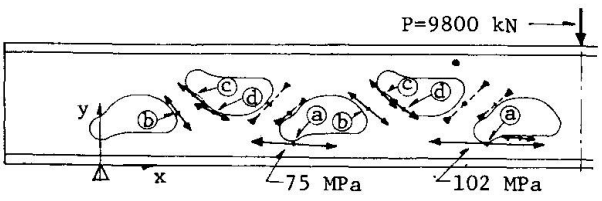

Fig.14 Principal stress distribution in the web of W-type beam.

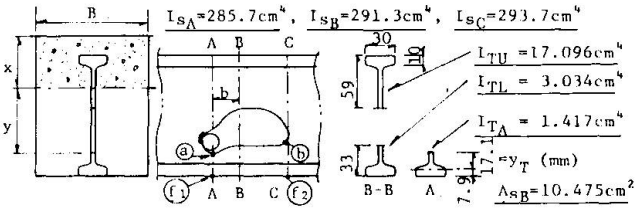

Fig.15 Cross sectional properties of the I-beam at a hole.

that the first crack would start at this point.
As a result of the detailed investigation, the following simplified formulas for normal stresses can be derived for the points ⓐ, ⓑ, ⓕ1 and ⓕ2 in Fig.15.

For an isolated I-beam,
$$\sigma_x = \alpha \frac{M}{I_S} \cdot y + \beta \frac{y_T}{I_T} \cdot \frac{I_{TL}}{I_{TU} + I_{TL}} \cdot b \cdot Q \qquad (1)$$

For an encased I-beam,
$$\sigma_x = \alpha \frac{M}{I_V} \cdot y + \beta \frac{y_T}{I_T} \cdot \frac{A_S}{\frac{B\,x}{n} + A_S} \cdot \frac{I_{TL}}{I_{TU} + I_{TL}} \cdot b \cdot Q \qquad (2)$$

where,
- α, β : the coefficients of stress concentration due to the web opening,
- b : the distance from the inflexion point of secondary bending moment at a hole due to shear force to the referring point, and is at the tests 2.5 cm and 5.5 cm for the points ⓐ, ⓕ1 and ⓑ, ⓕ2 , respectively,
- I_S, I_V : the moments of inertia of I-beam and composite beam at the referring cross section, respectively,
- I_{TU}, I_{TL} : the moments of inertia of the upper and lower T-sections at the inflexion point, respectively,
- I_T : the moment of inertia of the lower T-section at the referring point,
- y, y_T : the distance from the neutral axis to the referring point for the whole section and for the lower T-section, respectively,
- M : the bending moment at the referring point,
- Q : the shear force at the inflexion point,
- A_S : the cross sectional area of an I-beam at the inflexion point,
- B : the width of concrete section,
- x : the effective concrete depth at the inflexion point,
- n : the modular ratio of E_S/E_C.

The coefficients of stress concentration for each specimen and the above mentioned sectional properties are listed in Table 1 and in Fig.15, respectively. The coefficient at the bottom surface of the flange becomes 1.0 except in W-type. The value of β for W-type becomes 0.4 due to the effect of a diagonal portion of the web, because the behavior of W-type is similar to a Warren truss. The effect appears also on β-value at ⓐ. Comparing with the results obtained by FEM, proof of the accuracy of Eqs. (1) and (2) is shown in Fig.16 and 17. In a concrete -encased I-beam specimen, an amplitude of the zigzag strain distribution becomes smaller, because the concrete section can carry some part of the shear force as known in Eq.(2). Eq.(2) is also applicable to deck specimens. However, M and Q in the deck have to be deter-

Table 1 Coefficient of stress concentration

I-beam	Point	α	β
S	a	2.14	2.47
S-DB	b	1.08	1.95
	$f_{1,2}$	1.00	1.00
W	a	2.19	1.35
W-DB	a	2.10	1.52
W,W-DB	$f_{1,2}$	1.00	0.40

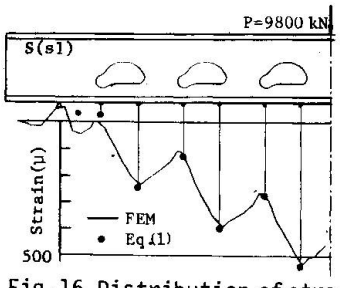

Fig.16 Distribution of strain on the bottom surface of S-type beam.

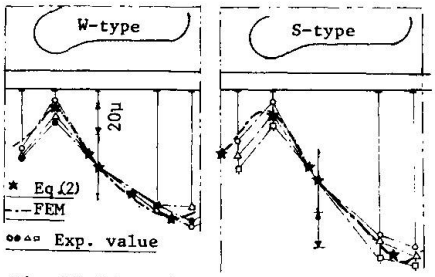

Fig.17 Distribution of relative strains on the bottom surface of the flange under a hole of an encased I-beam.

mined by an orthotropic plate theory. In a deck, since a wheel load is well distributed in the transverse direction, the influence of the second term in Eq.(2) becomes much smaller than that of encased beam specimen due to a decrease in the shear force.

3.3 S-N Relations

All the data from the fatigue tests and the resulting S-N curves obtained by the method of least square are shown in Figs.18 to 21. The vertical axis shows the magnitude of stress range at a cracking point given by the Eq.(1) or Eq.(2). Investigating these figures, the following features are able to be pointed out:

(1) From Fig.18, the effect of welding can be seen comparing features for S and W with those for S-DB and W-DB, respectively. The reduction of fatigue lives due to welding is remarkable. Especially, an abnormally large size tack welding gives worse results as seen in W-DB-type.

(2) Fig.19 is a diagram to show how long the remaining fatigue life is. It is worth to note that the remaining life after a crack has been initiated, is nearly equal to the initial crack life.

(3) The results from the deck tests are compared with the ones from the isolated I-beam tests in Fig.20. The test results in the decks, which are plotted at the fracture lives of I-beams, lie properly on S-N curves obtained for the fracture life of beam specimen within experimental errors. Such a good agreement gives the proof that M and Q in the decks can be evaluated accurately by the orthotropic plate theory. Also, the results from the deck tests have been modified considering cumulative damages due to the above mentioned multi-point loadings.

(4) The results in Fig.21 were prepared for discussions in the next section.

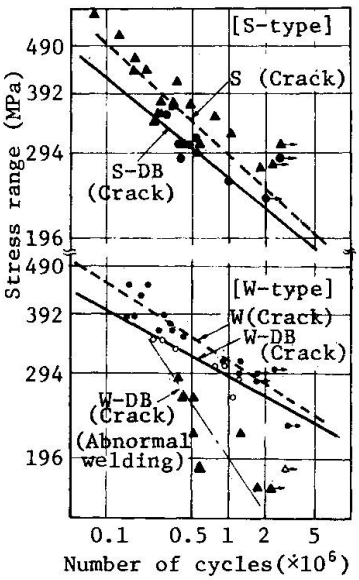

Fig.18 S-N relations for isolated I-beams.

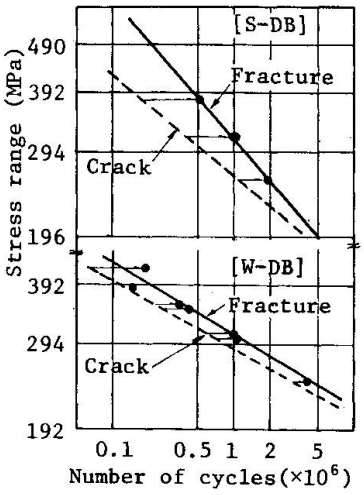

Fig.19 S-N relations for fracture life.

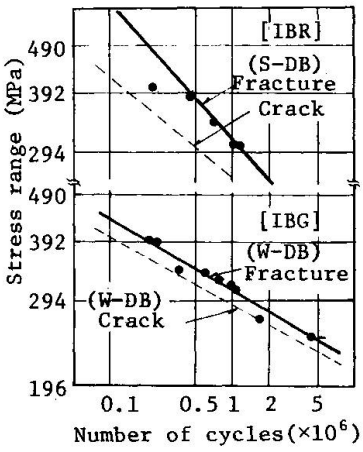

Fig.20 S-N relations for deck specimens.

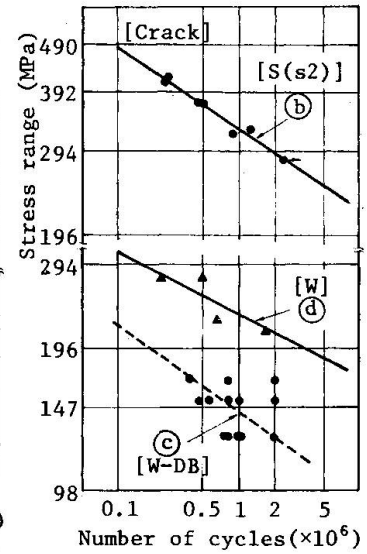

Fig.21 S-N relations at ⓑ in S-type, and at diagonal portions of web in W-type.

3.4 Fatigue Diagrams

It is difficult directly to find the difference between S-type and W-type in the S-N diagrams. Comparing these two types in term of fatigue diagrams, the difference is then clearly detected. The fatigue diagrams at 2×10^6 cycles are obtained using Eqs.(1) and (2) as shown in Fig.22. The results lead to the following discussions:

(1) Since W-type has more holes than S-type, the former has less stiffness than the latter. However, in reality, the fatigue strength of W-type is much larger than that of S-type. It depends on the decrease of α and β as discussed in Section 3.2.

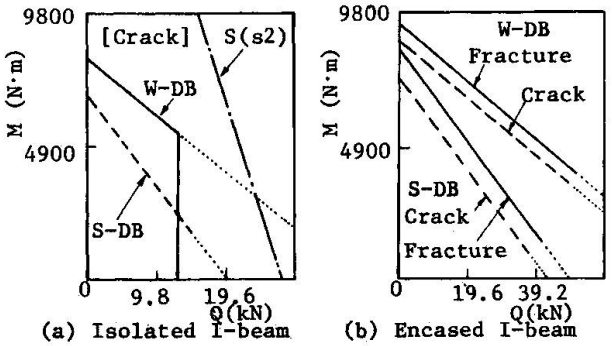

Fig.22 Fatigue diagrams at 2×10^6 cycles.

(2) One limit of the values of shear force exists in an isolated I-beam of W-type. In case the shear force becomes larger than the limit, a crack will occur in a diagonal portion of the web.
(3) The fatigue strength at the point ⓑ in S(s2)-type is much larger than that at the point ⓐ in S-type. Therefore, if an I-beam has holes facing in the same direction, the first crack will be sure to be initiated at the point ⓐ.
(4) Even though the fracture life is two times as large as the crack life, the difference of fatigue diagrams between fracture and crack is not so large.
(5) The effect of concrete on the fatigue life is extremely great. It depends not only on stresses decreasing due to the composite action, but also on a decrease in shear force due to a share with concrete.

4. EVALUATION OF FATIGUE SAFATY OF ACTUAL FLOORS

4.1 Procedure for Derivation of Safety Factor

Using the above mentioned S-N curves, it is possible to evaluate the fatigue safaty of actual floors under traffic load. Now, the fatigue safety of five decks, of which the span length are 1.5, 2.0, 2.5, 3.0 and 3.5 m, is derived under the combination of the following conditions: (a) Employed I-beam: S-DB and W-DB, (b) Traffic load spectrum: two actually measured spectra of rear axle loads of NHW and UEW as listed in Table 2, where, NHW means a spectrum on a national highway in Japan and UEW means one on an urban expressway in Japan[5]. (c) Probability functions of passing positions of vehicle wheels on a road surface: two actually measured functions of NHW and UEW as shown in Table 3. (d) Daily traffic volumes of vehicles on a single lane: 10,000, 15,000 and 20,000. (e) Design life of bridges: 50 years.

Table 2 Axle load spectra

Weight (kN)	NHW (%)	UEW (%)
0 ~ 20	73.03	79.54
20 ~ 39	10.61	9.60
39 ~ 59	8.09	6.16
59 ~ 78	3.32	2.21
78 ~ 98	2.12	1.35
98 ~118	1.60	0.78
118 ~137	0.849	0.238
137 ~157	0.210	0.079
157 ~176	0.091	0.028
176 ~196	0.038	0.028
196 ~235	0.034	0.012
235 ~274	0.0071	0.006
274 ~314	0.00092	-----

Table 3 Probability function of passing position of vehicles

	Mean value	Standard deviation	L=width of one lane
NHW	0.73 L	0.09 L	Left wheel, Right lane mark
UEW	0.77 L	0.065 L	

The fatigue safety is evaluated by the following processes: (a) Calculate N_{eq} of Eq.(3) based on the Miner's linear damage hypothesis. (b) Find the fatigue stress (σ_f) corresponding to the cycles N_{eq} on a S-N curves. (c) Obtain the maximum stress (σ_d) acting at a referring point under a specified axle load including impact with a plate analysis. (d) Finally calculate the safety factor given by the ratio of σ_f to σ_d. Fig.23 is a block diagram of the procedure for the explanation.

$$N_{eq} = N_t \int_{T_{min}}^{T_{max}} \left(p(T) \cdot \left(\frac{T}{156.8}\right)^{1/K} \right) dT \cdot \int_0^L \left(p(x) \cdot Inf(\sigma)^{1/K} \right) dx \quad (3)$$

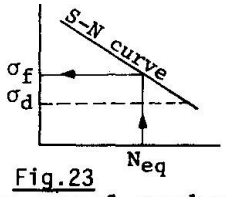

Fig.23

where,
N_{eq} : the effective number of cycles which is converted from the total number of traffic loading cycles N_t by the cumulative damage law,
N_t : (design life in year of the bridge) × 365 days × (daily traffic volume),
T : the rear axle load of a vehicle in the unit of kN,
156.8 : the specified rear axle load in the unit of kN,
p(T) : the axle load spectrum,
p(x) : the probability function of passing position of wheels,
Inf(σ) : the influence value of stresses along a referring I-beam with regard to a referring point,
K : the absolute value of a slope of a S-N curve.

4.2 Results, Discussions and Recommendations

Discussions on the fatigue safety have to be done with optimum cross sections

designed by the conventional formula[2]. Table 4 gives an optimized design cross section of each deck. The maximum design stress in the bottom flange of I-beams is almost equal to the allowable stress. Figs.24 to 26 show the resulting safety factors regarding the referring point apart 10 cm from the midspan of each deck. Each figure leads to the following discussions:

(1) Generally, W-type seems to have sufficient fatigue strength as seen in Fig.24. S-type is not suitable for a deck whose span is less than 2.3 m.

(2) Both load spectra and daily traffic volumes significantly influence on the safety. Therefore, NHW spectrum still has to be used for the assessment of fatigue. The daily traffic volume of 20,000 is probably the largest in Japan. However, it may be desirable to use the number for the fatigue design of decks.

(3) Two safety curves associated with the fracture life and crack life are illustrated in Fig.26 for a comparison. The difference between the two safety factors can not be observed in S-type, because the slope of the S-N curve for the fracture life becomes larger than that for the crack life. So, in an actual design it seems to be desirable to use the crack life even for W-type.

Table 4 Cross section of decks and design stress

	Span length				
	1.5m	2.0m	2.5m	3.0m	3.5m
t (cm)	16	17	18	19	20
B (cm)	28.5	23.5	19.5	17.0	15.0
σ (MPa)	133	136	137	136	137

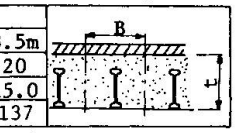

σ_a=137.2 MPa

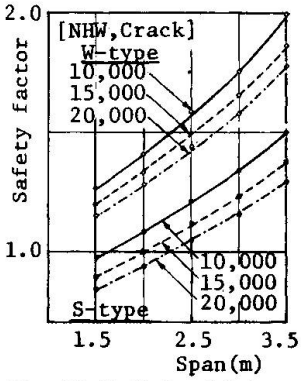

Fig.24 Safety factors for crack life.

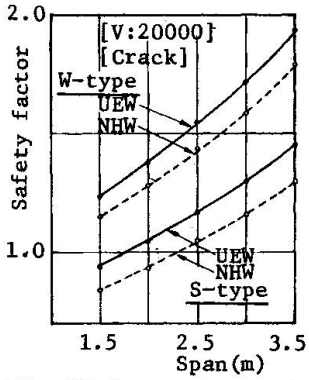

Fig.25 Comparison of load spectra used for safety factor.

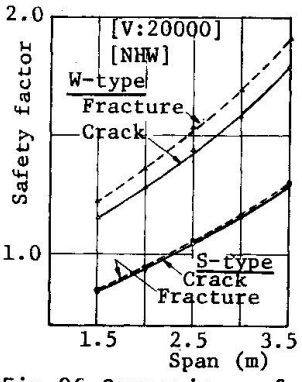

Fig.26 Comparison of fatigue life used for safety factor.

5. CONCLUSIONS

Through three of tests, the effect of cracks and the fatigue safety of Concrete Filled Grating Floors were made clear. The followings are concluded from the present study:

(1) Fatigue strength of the floors is governed by that of encased I-beams.
(2) I-beams of W-type are more reliable than those of S-type.
(3) The floors designed by the present design method have generally sufficient fatigue strength.
(4) The fatigue safety of the floors is influenced by vehicle loads, position spectra, and traffic volumes.
(5) The fatigue safety of the floors has to be evaluated by the initiation lives of cracks
(6) Eqs.(1) and (2) are useful stress formulas for I-beam having holes.

REFERENCES

1. Y.MAEDA and S.MATSUI: Experimental Study on Structural Behaviors and Load-Carrying Capacity of Full-Sized Steel Grating Floors, Trans. of JSCE, 1978.
2. JRA: Design Manual for Steel Highway Bridges, Japan Road Association, 1979. *(in Japanese)*
3. The Surveying Committee for Highways: Rept. on the Design and Construction of I-beam Grating Floors, Japan Road Public Corporation, 1980. *(in Japanese)*
4. S.MATSUI and Y.MAEDA: Structural Behaviors and Design of Concrete Filled Steel Grating Floors, 1st Annual Conf. of JCI, 1979. *(in Japanese)*
5. T.KUNIHIRO et al.: Study on Design Live Loads - Actual Traffic Loads and Application to Bridge Design -, Rept. of the Public Works Reseach Institute, Minst. of Const., 1971. *(in Japanese)*